PHYSICALLY REALISTIC MODELS OF CATASTROPHIC BUBBLE COLLAPSES

Brian D. Storey[1], Hao Lin[2], & Andrew J. Szeri[2]

1. Franklin W. Olin College of Engineering, Needham, MA 02492-1245, USA.
2. University of California at Berkeley, Department of Mechanical Engineering, Berkeley, CA 94720-1740, USA.

Abstract

When gas micro-bubbles are forced with an acoustic field they typically undergo a slow expansion followed by a violent collapse. During the expansion phase a significant amount of vapor enters the bubble. While much of this vapor is expelled as the bubble collapses, significant excess vapor is trapped in the interior during this violent collapse. As the bubble collapses this vapor is significantly heated and undergoes dissociative chemical reactions. Applications which take advantage of these acoustically driven chemical reactions are generally known as sonochemistry. Using the results of direct numerical simulations as a base, reduced models of the transport and gas dynamics of this sonochemical process are carefully developed. The models are compared to experimental data, showing that the reduced formulations can be used to predict real phenomena.

1 Introduction

Sonochemistry is a chemical processing technique that derives from the violent oscillations of acoustically driven micro-bubbles. The non-linear radial oscillations typically have a slow expansion followed by a violent collapse. The collapse is so rapid that the temperature in the bubble interior can reach several thousand Kelvin and several thousand atmospheres. These extreme, localized conditions drive chemical reactions that can be used for a variety of applications, which we will briefly discuss.

Sonochemistry can be used to manufacture protein micro-spheres. These hollow, micron-sized protein shells are formed when chemical reactions occurring in the gas phase cause proteins on the bubble interface to permanently cross-link. The micro-spheres can be injected into the bloodstream to act as contrast agents in ultrasonic imaging. Alternately, the spheres can be manufactured with a liquid interior and used for drug delivery (Suslick *et al.* 1999).

The rapid heating and cooling rates in sonochemistry can create nano-phased amorphous metals that have unusual magnetic, electric, and catalytic properties (Suslick *et al.* 1999). Sonodynamic medical therapy has been experimented with as a method for targeted tumor destruction. The ultrasonically induced cavitation can activate porphyrins: drugs that act as anti-tumor agents when irradiated. Ultrasound is able to target precise areas deep in the tissue, minimizing damage to surrounding, healthy tissue (Umemura *et al.* 1996). Further, sonochemistry has been used in the chemical remediation of water with some success (Mason 1999).

In some applications sonochemical effects may be undesirable. For example, in shockwave lithotripsy a shock wave is sent into the body to destroy kidney stones. A typical shock pulse has a strong positive pressure shock front followed by a long negative pressure tail. The negative pressure can cause air micro-bubbles in the blood and tissue to grow to millimeter size before undergoing a free collapse. Radicals generated on the collapse have an unknown side effect on healthy tissue (Matula *et al.* 2000).

This paper will emphasize the development of reduced models for the gas dynamics and transport within the collapsing bubble: models that capture the essential physics but are much more efficient than detailed simulations. The work will focus on the importance and coupling of heat and mass transfer in the sonochemistry process, emphasizing the role that phase change and subsequent diffusion of vapor play in understanding trends in sonochemistry data.

2 Formulation

One approach we have taken to studying the gas dynamics in acoustic cavitation has been direct numerical simulation (DNS) of one-dimensional gas dynamics. The formulation has included heat transfer, mass transfer, phase change, chemical reactions, and thermal diffusion (Storey & Szeri 2000). This approach has the disadvantage of requiring extensive computation that prohibits parameter studies, optimization, and multi-bubble modeling. The second approach takes an "averaged" viewpoint: the full partial differential equations governing the gas motion are integrated over the volume and approximations are made for the boundary terms in the equations (Storey & Szeri 2001). The result is a set of ordinary differential equations, representing a more practical tool for computing multi-bubble applications. The validity of assumptions that go into such reduced models are, however, largely unknown. A variety of other approaches that vary in method and assumptions have been used for this problem (For example, Colussi *et al.* (1998), Gong & Hart (1998), Moss *et al.* (1999), Prosperetti *et al.* (1988)).

2.1 Gas dynamics in the bubble interior

Most studies of bubble dynamics rely upon the Rayleigh-Plesset equation (RPE): a non-linear ODE derived from the Navier-Stokes equations in the liquid. While the RPE describes the motion of the liquid, the equation must couple to the gas behavior where an assumption of uniform gas pressure is common. Conventional understanding is that the uniform pressure assumption (and therefore the RPE) breaks down during violent cavitation phenomena since the bubble collapse reaches supersonic Mach numbers (Lin *et al.* 2000).

A simple analysis can show that the pressure variation in the bubble is intimately connected to the acceleration of the bubble wall, not the velocity. Analysis of the momentum conservation equation shows that the pressure variation in the bubble follows a quadratic form with the magnitude of the pressure difference given as:

$$\epsilon_P \equiv \frac{\bar{\rho}\ddot{R}R}{2P_C} = \frac{P_C - P_W}{P_C}, \tag{1}$$

where $\bar{\rho}$ is time dependent average density, R is the bubble radius, P_C is the pressure at the center, P_W is the pressure at the wall, and dot denotes time derivative (Lin *et al.* 2000).

A formal analysis can show that the above representation for the pressure field is valid even in extremely violent collapses (Lin *et al.* 2000). Rather than show a lengthy analysis here, Figure 1 will be used to demonstrate the validity of this approach. Figure 1 shows the Mach number of the collapse (around the time of minimum radius), the value of $\bar{\rho}\ddot{R}R/2P_C$, and and the value of $(P_W - P_C)/P_C$ where the pressures are taken from the DNS. The agreement between the analytical expression and DNS is striking, given that the peak Mach number is very high. Extensive comparisons of this simple result under a variety of conditions show excellent agreement in all cases.

This result is important in models of violent cavitation as it shows precisely when the uniform pressure approximation is valid and provides a methodology to compute the pressure variation in the gas in a simple, reasonable way (i.e without solving the PDE for momentum conservation).

2.2 Heat transfer approximations

To differentiate between the effects of heat and mass transfer we will first look at the case where the vapor pressure of the liquid is zero and therefore mass transfer of vapor will not play a role. This example is only meant to isolate the influence of heat transfer. In the spirit of the previous section, we will use the detailed numerical simulations to test the assumptions of reduced heat transfer models.

In Figure 2 we show the instantaneous energy contained in the bubble, the total amount of heat loss, and the total work done by the bubble. We see that the total heat and work (done by the gas) are equal well before the collapse, representing isothermal behavior. Around the time of minimum radius, the energy of the contents suddenly rise in the bubble interior while the total heat loss is relatively small compared to the amount stored (nearly adiabatic behavior). It is easy to see that there is some heat loss through the collapse (Storey & Szeri 2000).

A reduced model of heat transfer can be developed based on competition of time scales. When the bubble is moving fast relative to the time it takes heat to diffuse from the center of the bubble to the wall, the

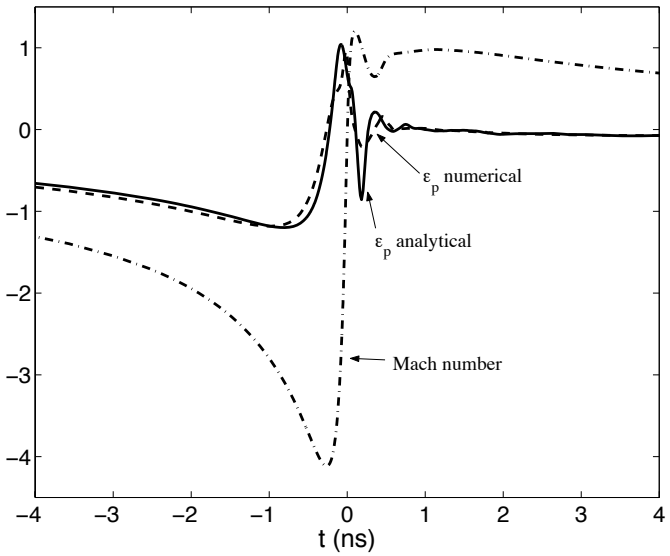

Figure 1: The Mach number of the collapse, the pressure difference parameter from DNS pressures $(P_W - P_C)/P_C$, and the pressure difference parameter from analysis $\bar{\rho}R\ddot{R}/P_C$. The time dependent parameter ϵ_P captures the real behavior of the pressure field computed from DNS. The case is argon dissolved in water, P_A=1.25 atm, R_0=4.5μm, ω=26.5 kHz. Time is centered when the collapse reaches minimum radius.

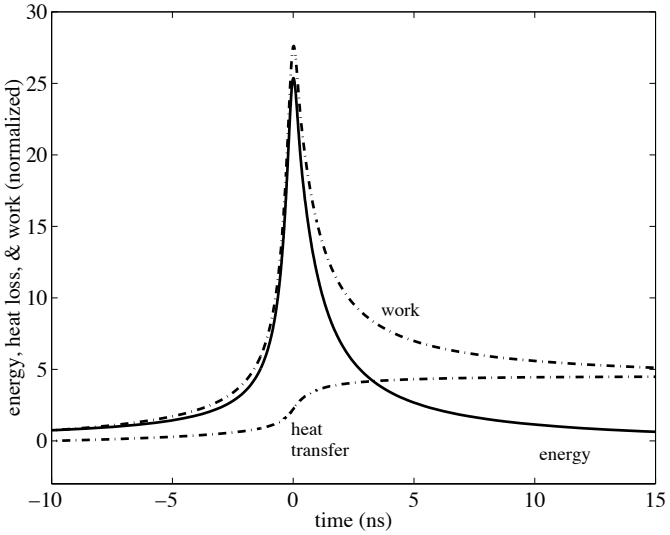

Figure 2: The total instantaneous energy contained in the gas, compared to the total amount of heat loss and the work done by the gas (first law of thermodynamics). The energy is scaled by P_0V_0, where P_0 and V_0 are the pressure and volume of the bubble at its ambient state. The case is argon dissolved in water, P_A=1.25 atm, R_0=4.5μm, ω=26.5 kHz. Time is centered at the time of minimum radius.

bubble behaves approximately adiabatically. When the bubble moves slow compared to the heat transfer time, the bubble is able to remain in thermal equilibrium with the ambient liquid. The dynamic time scale $R/\dot{R}$ equals the diffusive time scale R^2/α (α is thermal diffusivity) at -7 and 10 ns, relative to the time of

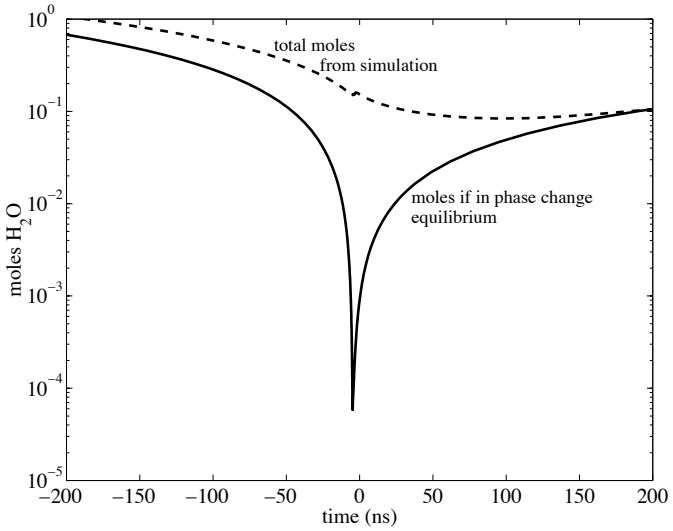

Figure 3: The total number of moles of vapor trapped in the bubble compared to the amount if phase change equilibrium could be maintained. The moles of water are scaled by the total number of moles contained in the bubble at the initial state. The case is argon dissolved in water, P_A=1.25 atm, R_0=4.5μm, ω=26.5 kHz. Time is centered at the time of minimum radius.

minimum radius (Storey & Szeri 2001).

2.3 Mass transfer approximations

The understanding of mass transfer is perfectly analogous to heat transfer. When the bubble motion is slow compared to the time it takes a vapor molecule to move from the bubble center to the bubble wall, the vapor fraction is uniform within the bubble interior (analogous to isothermal behavior). When the relative bubble motion is fast, the vapor has insufficient time to diffuse out of the bubble and there is nearly a constant mass process (analogous to adiabatic behavior). Further, through much of the cycle the conditions are changing rapidly enough that the bubble interface is not in equilibrium: one can compute the rate of phase change from kinetic theory. Conventional models typically neglect both the finite rate of transport inside the bubble as well as the limited rate of phase change (Storey & Szeri 2000).

In Figure 3 we show the total number of moles in the interior of the bubble compared to the number *if* the bubble interface was in perfect phase change equilibrium and mass transfer was infinitely fast (a common implicit assumption in the RPE). Two features are immediately obvious: one is that the finite rate of phase change results in more vapor trapped in the bubble interior throughout the part of the cycle even when the distribution is uniform in the bubble interior (before -50 ns). More striking is that mass transfer within the bubble is too slow to allow the vapor to diffuse out of the bubble when the gas pressure is high at collapse. If one does not account for mass transfer and phase change, an insignificant amount of vapor is contained in the bubble at collapse. The trapped vapor has a major impact on the prediction of peak temperatures and is usually the source of "fuel" for sonochemical activity (Storey & Szeri 2001).

2.4 Heat and mass transfer

The previous two sections were meant to show the effects of heat and mass transfer, as though the two effects could be treated independently. In reality the two processes are linked together and the must be considered simultaneously (Storey & Szeri 2001).

To demonstrate this point consider a mixture of argon and helium dissolved in water and "measure" the change in chemical production as the gas mixture composition is varied. The experimental data has a

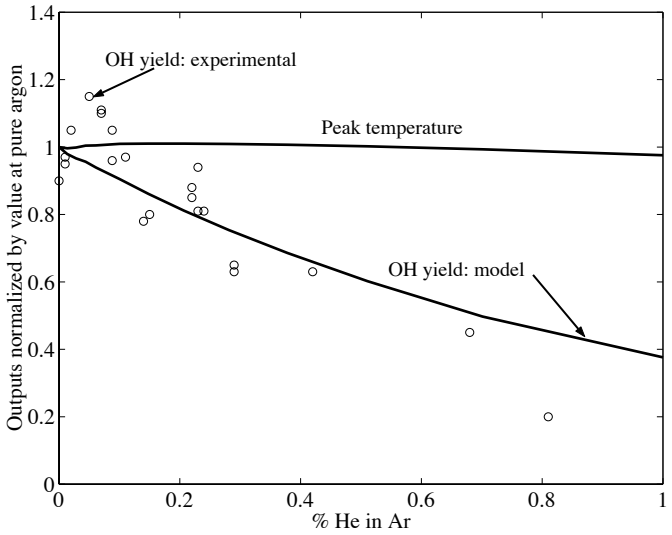

Figure 4: The normalized (by pure Ar case) OH yield and peak temperature as the gas contents are changed from Ar to He. Case is P_A=2.0 atm, R_0=4.5μm, ω=300 kHz. Pure Ar temperature is 4525 K. The experimental data were taken from Mark *et al.* (1998)

general trend of the sonochemical yields decreasing as the composition of the gas mixture is changed from pure argon to pure helium. This trend has been traditionally explained as a result of more heat loss: helium has a high thermal conductivity.

We find that the realistic case is complicated by the coupling between heat and mass transfer. Since helium has a higher mass diffusivity, less water is trapped in a helium bubble. Less vapor means higher temperatures are possible since the vapor has a low ratio of specific heats and gets caught in endothermic chemical reactions. On the other hand helium does have a higher thermal conductivity, promoting more heat loss. These two effects compensate one and other and result in only minor changes in peak temperature as the gas composition changes. On the other hand if vapor is neglected then the temperature changes are quite dramatic, with helium being significantly colder than argon. Given that heat and mass transfer are analogous, this compensating effect is not very surprising.

In Figure 4 we show the normalized OH yield and peak temperature as the gas composition is varied. Consistent with the above explanation, the OH yield decreases while the temperature does not change much. The OH yields have a similar trend as the experimental data, given the uncertainties involved.

3 Modeling of applications

In order to demonstrate that these models can be used to understand real physical phenomena we include two brief examples. These examples show that the simplified single bubble model is able to explain the general phenomena. To model these phenomena we will use the reduced model of gas dynamics, heat transfer, and mass transfer presented in the previous section. The models will be shown to be useful in explaining and predicting real sonochemistry phenomena.

3.1 Sonochemistry of methanol-water mixtures

We now consider the case of a more general and complicated chemical system than the previous examples. As an example we consider the case where the liquid is a water-methanol mixture of varying composition. We use all the previous methods as before with a minor modification: a new reaction mechanism is used

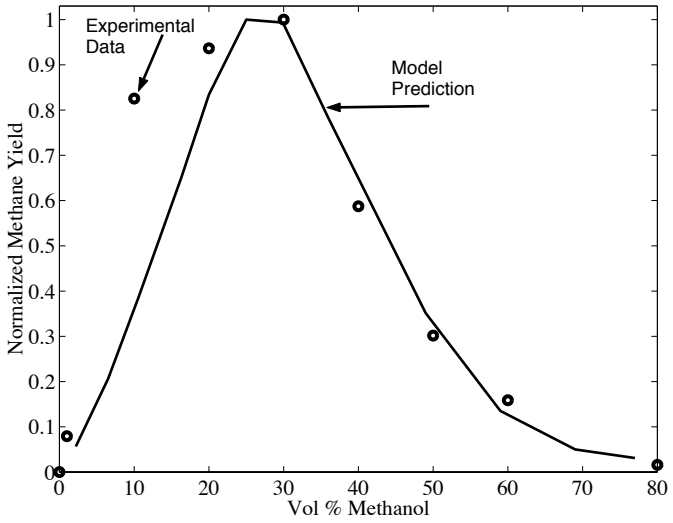

Figure 5: The normalized sonochemical yield of methane as the liquid composition (water-methanol mixture) is varied. The parameters used were P_A=2.5 atm, R_0=4.5μm, ω=321 kHz. The experimental data is from Eulaerts *et al.* (2000).

that accounts for methanol chemistry and liquid-vapor equilibrium data for mixtures is used to relate vapor composition to the liquid composition.

The modifications are straightforward and the reduced model is able to predict the sonochemical yields as the composition of a methanol-water mixture is varied. Figure 5 shows the sonochemical production of CH_4 as the liquid composition of the water-methanol mixture varies. The general trend is relatively easy to understand. At zero methanol composition, no methane can be formed since there is no carbon in the system. As the methanol fraction increases, there are more carbon atoms in the trapped vapor phase and therefore more "fuel" for the CH_4 production. On the other hand, methanol has a very high vapor pressure, so as the methanol composition increases excessive methanol vapor is trapped by the collapse. More methanol vapor trapped at collapse means lower temperatures: methanol has a low ratio of specific heats and undergoes many endothermic dissociation reactions. These lower temperatures result in less dissociation and therefore eventually less CH_4 production. Therefore, there are a competing effects: the availability of "fuel" for CH_4 production and lower collapse temperatures. These competing effects find an optimum at some water-methanol composition.

3.2 Shockwave lithotripsy

Shock wave lithotripsy (SWL) is a well known method for destroying kidney stones with a series of intense, focused shock waves. The pressure pulse typically has a strong positive pressure shock front followed by a long negative pressure tail. This negative pressure tail causes small bubbles in tissue and blood to grow rapidly and expand to large volumes. Long after the shock and pressure tail have passed, the bubble continues to grow by inertia until it finally halts and begins to undergo a violent, free collapse.

Figure 6 shows the radial dynamics of a bubble responding to a SWL pulse. The jagged line is experimental data while the smooth line is a simulation using the assumptions presented within this paper. Models without heat and mass transfer are not able to even approximate the dynamics of these violent oscillations. The bubble takes in enormous amounts of water vapor as it expands from micron to millimeter size. On the collapse, much of this vapor is retained and the bubble has approximately 2,000,000 times more vapor than gas molecules. Without the vapor one cannot predict the long afterbounces or the peak temperature of the collapse.

In order to "fit" the experimental data there is only one unknown parameter: the absolute amplitude of

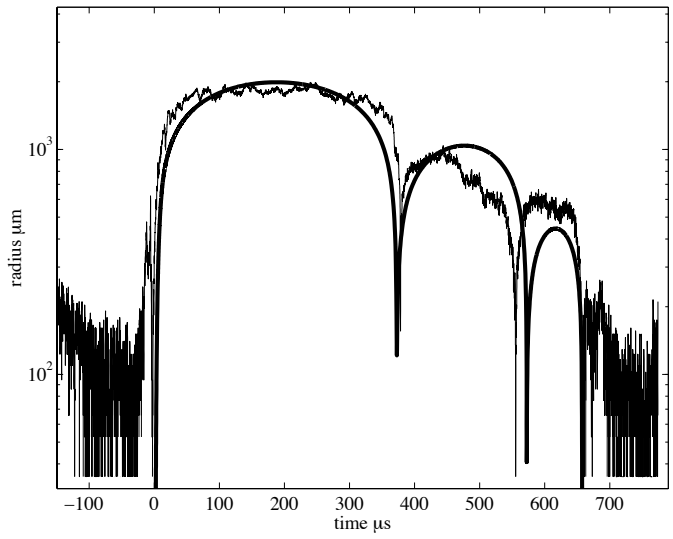

Figure 6: The radial response of a bubble to a shock wave lithotripsy pulse. The jagged line is experimental data compared to the smooth curve from the model. The pulse has ω=50kHz, P_A=250 atm, and β=30kHz. Experimental data are taken from Matula (2000).

the pressure pulse. The shape of the pulse is known from experiments, but the absolute amplitude at the location of the bubble is not. The initial size of the bubble does not influence the dynamics, as the dynamics are dominated by the vapor in the bubble. By simply varying the amplitude of the pressure pulse, one can match the experimental radial dynamics to the model and therefore "back out" the amplitude of the pressure pulse.

4 Conclusions

We have presented results validating the assumptions made in single bubble models of violent cavitation. Using direct numerical simulation we are able to directly evaluate simplified and practical models. We have shown that the pressure non-uniformity in the bubble can be taken into account without numerically solving the momentum equation. We have also shown that scaling arguments for heat and mass transfer can give reasonable approximations.

These simplified models are shown to predict trends in sonochemistry data upon variation of gas and liquid composition. While these are only single bubble models, the trends are similar to experiments and the models give insight into what is controlling sonochemical output. Further, the violent radial dynamics of bubbles in SWL are well modeled by these methods.

References

[1] Colussi, A.J., Weavers, L.K., & Hoffmann, M.R. 1998 Chemical bubble dynamics and quantitative sonochemistry. *J. Phys. Chem. A* **102**, 6927–6934.

[2] Colussi, A.J. & Hoffmann, M.R. 1999 Vapor Supersaturation in Collapsing Bubbles. Relevance to the Mechanisms of Sonochemistry and Sonoluminescence *J. Phys. Chem.* **103(51)**, 11336-11339.

[3] Gong, C. & Hart, D.P. 1998 Ultrasound induced cavitation and sonochemical yields. *J. Acoust. Soc. Am.* **104**, 2675–2682.

[4] Lin, H., Storey, B.D., & Szeri A.J. 2000 Inertially driven pressure inhomogeneities in violently collapsing bubbles: the validity of the Rayleigh-Plesset equation. *J. Fluid Mech.* in review.

[5] Mason, T.J. 1999 Sonochemistry: current uses and future prospects in the chemical and processing industries. *Phil. Trans. R. Soc. Lond. A* **357**, 355–369.

[6] Mark, G., Tauber, A., Laupert, R., Schechmann, H.-P., Schulz, D., Mues, A., & von Sonntag, C. 1998 OH-radical formation by ultrasound in aqueous solution - Part II: Terephthalate and Fricke dosimetry and the influence of various conditions on the sonolytic yield. *Ultrason. Sonochem.* **5** 41–52.

[7] Matula, T.J. Acoustic cavitation and sonoluminescence. 2000. J. Acoust. Soc. Am. **108**, 2492.

[8] Moss, W.C., Young, D.A., Harte, J.A., Levatin, J.L., Rozsnyai, B.F., Zimmerman, G.B., & Zimmerman, I.H. 1999 Computed optical emissions from a sonoluminescing bubble. *Phys. Rev. E*, **59** 2986–2992.

[9] Prosperetti, A., Crum, L.A., & Commander, K.W. 1988 Nonlinear bubble dynamics. *J. Acoust. Soc. Am.* **83**, 502–514.

[10] Storey, B.D. & Szeri, A.J. 2000 Water vapour, sonoluminescence, and sonochemistry. *Proc. R. Soc. Lond.*, **456** 1685–1709.

[11] Storey, B.D. & Szeri, A.J. 2001 A reduced model of cavitation physics for use in sonochemistry *Proc. R. Soc. Lond.*, to appear.

[12] Suslick, K.S., Didenko, Y., Fang, M.F., Hyeon, T., Kolbeck, K.J., McNamara, W.B., Mdleleni, M.M., & Wong, M. 1999 Acoustic cavitation and its chemical consequences. *Phil. Trans. R. Soc. Lond. A* **357**, 335–353.

[13] Umemura, S., Kawabat, K., Sasaki, K., Yumita, N., Umemura, K., Nishigaki, R. 1996 Recent advances in sonodynamic approach to cancer therapy. *Ulta. Sonochem.*, **3**, 187–191.